

# Tripartite entanglement and Bell non-locality in loop-induced Higgs boson decays

**Roberto A. Morales**

[roberto.morales@fisica.unlp.edu.ar](mailto:roberto.morales@fisica.unlp.edu.ar)

Based on **EPJ C 84 (2024) 6, 581**



UNIVERSIDAD  
NACIONAL  
DE LA PLATA

**Quantum Observables for Collider Physics**  
7-10 April 2025 – GGI Florence

# Outline

- Introduction
- Three-body Higgs boson decays  $H \rightarrow \gamma l\bar{l}$
- Entanglement quantifiers for 3-qubit states
- Related bipartite Higgs decays
- Numerical results
- Summary and perspectives

# Introduction

## High-energy colliders as “quantum information laboratories”

Significant progress mainly focuses on quantum properties in bipartite systems:  
top-pair, diboson production,  $H \rightarrow VV^*$ , tau-pair, VBS, single-top, neutrinos,  $B$ ,  $K$ , ...  
BSM (SMEFT, anomalous couplings, ...), Fundamental Principles (MaxEnt, Area Law, ...)

### ATLAS and CMS measurements for $t\bar{t}$ production

[Nature 633 (2024) 542; Rept. Prog. Phys. 87 (2024) 117801; PRD 110 (2024) 11, 112016]

Deeper understanding of multipartite correlations is needed.  
Crucial not only for make progress fundamental physics but also for  
developing emerging quantum technologies.

Systematic investigations of three-particle entanglement and non-locality  
in particle physics is underexplored [Aein et al., Sakurai et al.; Subba et al.; Fonseca et al.; Quinta et al.;  
Blasone et al.; Konwar et al.; Aguilar-Saavedra; Bernal et al.; RAM]

# Extending to multi-particle states

Three-body Higgs decay  $H(p_H) \rightarrow \gamma(k) l^-(p_-) \bar{l}^+(p_+)$  as a case study

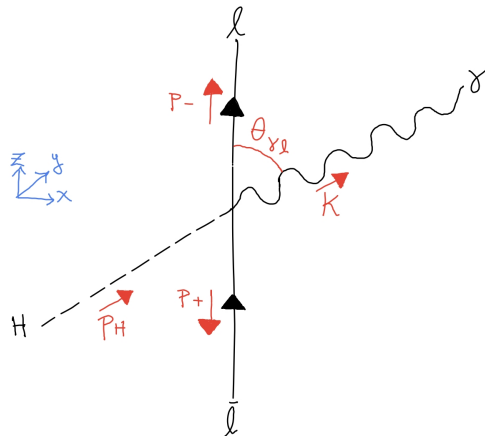
Proposals to study CP properties of the Higgs boson and BSM theories.

Related to bipartite Higgs decaying into  $\gamma\gamma$  and  $\gamma Z$ .

13 TeV data: ATLAS evidence below 30 GeV and CMS  $\sigma$  bounds at  $Z$ -peak.

[PLB 819, 136412 (2021)]

[JHEP 11, 152 (2018)]



# Goals and approach

## Detailed theoretical predictions for quantum properties of this exotic Higgs decay

- Identify relevant kinematical regions with high degree of entanglement.
- Quantify deviations from local realistic predictions in the phase space.

### Caveat

Very low statistics and lacking of techniques to measure spin of stable particles.

### Plan

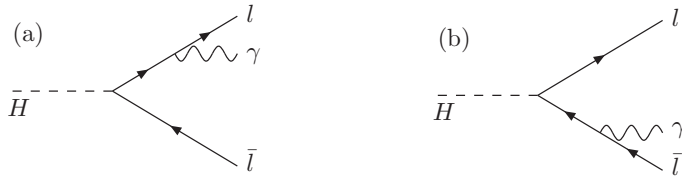
Compute the helicity amplitudes  $\mathcal{M}_{s_1 s_2 s_3}$  of three-body Higgs decays.

Arrive to the full knowledge of  $\rho$ .

Define quantifiers related to entanglement detection and test Bell non-locality.

# Three-body Higgs boson decay at tree level

SM modified by  $\tilde{\mathcal{L}}_{HII} = -\frac{Y_I}{\sqrt{2}} \kappa_{CP}^I H \bar{\psi}_I (\cos \delta_{CP}^I + i \gamma^5 \sin \delta_{CP}^I) \psi_I$  ( $I = e, \mu, \tau$ )

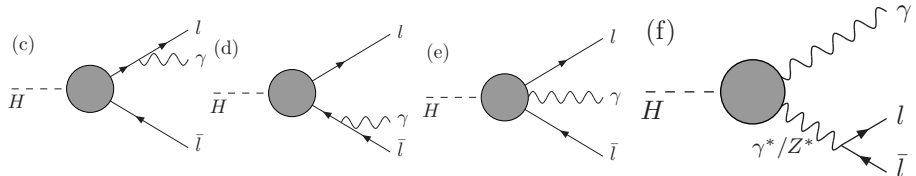


$$\mathcal{M}_{s_1 s_2 s_3}^{\text{Tree}} = e \frac{Y_I}{\sqrt{2}} \kappa_{CP}^I \bar{u}_{s_2} \left( \frac{(\not{q}_{s_1}^* \not{k} + 2\varepsilon_{s_1}^* \cdot p_-)(\cos \delta_{CP}^I + i \gamma^5 \sin \delta_{CP}^I)}{2k \cdot p_-} - \frac{(\cos \delta_{CP}^I + i \gamma^5 \sin \delta_{CP}^I)(\not{k} \not{q}_{s_1}^* + 2\varepsilon_{s_1}^* \cdot p_+)}{2k \cdot p_+} \right) v_{s_3}$$

Two relevant kinematical variables in the dilepton rest frame:  
 dilepton invariant mass ( $m_{l\bar{l}} = \sqrt{s}$ ) and the polar angle between photon and lepton ( $\theta_{\gamma l}$ )

**CP-effects here and Yukawa suppressed amplitude**

# Three-body loop-induced Higgs boson decay



$$\mathcal{M}_{s_1 s_2 s_3}^{1\text{-loop}} = \bar{u}_{s_2} \left( (\varepsilon_{s_1}^* \cdot p_- \not{k} - k \cdot p_- \not{\epsilon}_{s_1}^*) (\textcolor{brown}{a}_1 P_R + \textcolor{brown}{b}_1 P_L) + (\varepsilon_{s_1}^* \cdot p_+ \not{k} - k \cdot p_+ \not{\epsilon}_{s_1}^*) (\textcolor{brown}{a}_2 P_R + \textcolor{brown}{b}_2 P_L) \right) v_{s_3}$$

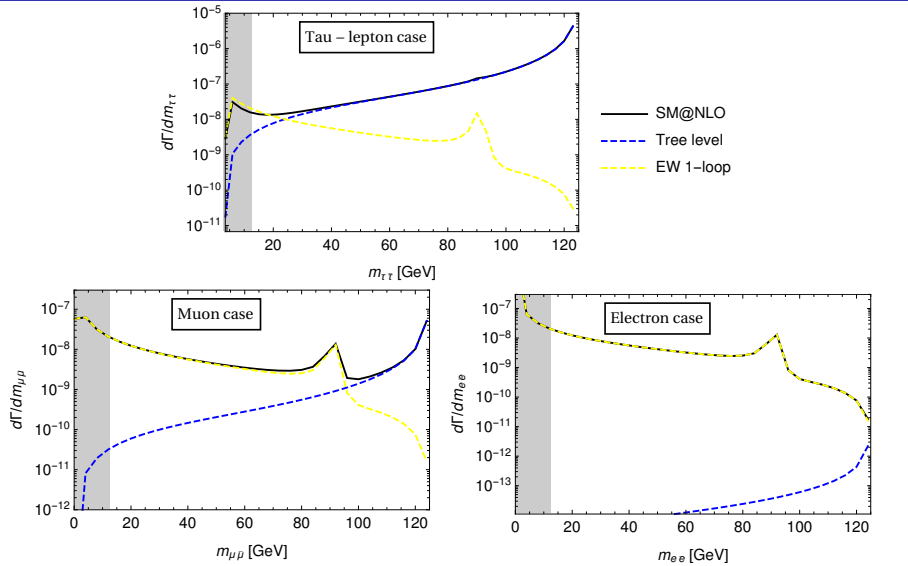
SM form factors from Kachanovich et al. [PRD 101, 073003 (2020)]

No Yukawa suppression nor CP-effects here (in contrast to tree-level)

**Unique opportunity to examine quantum correlations from radiative corrections**

[see also Severi et al.; Grossi et al.]

# Tree vs Loop contributions



$$\frac{d\Gamma_{H \rightarrow \gamma l\bar{l}}}{dm_{l\bar{l}} d\cos(\theta_{\gamma l})} = \frac{\sqrt{s - 4m_l^2(m_h^2 - s)}}{256\pi^3 m_h^3} \sum_{s_1, s_2, s_3} |\mathcal{M}_{s_1 s_2 s_3}|^2 \quad \text{where } (0.1m_h)^2 \leq s = m_{l\bar{l}}^2 \leq s_{\text{cut}} = m_h^2 - 2m_h E_{\text{cut}}^\gamma$$

## 3-qubit formalism

8×8 density matrix  $\rho$  in terms of the helicity amplitudes

$$\langle s_1 s_2 s_3 | \underbrace{\psi\rangle\langle\psi|}_{\rho} \tilde{s}_1 \tilde{s}_2 \tilde{s}_3 \rangle = \left( \sum_{s_1, s_2, s_3} |\mathcal{M}_{s_1 s_2 s_3}|^2 \right)^{-1} \mathcal{M}_{s_1 s_2 s_3} \mathcal{M}_{\tilde{s}_1 \tilde{s}_2 \tilde{s}_3}^\dagger$$

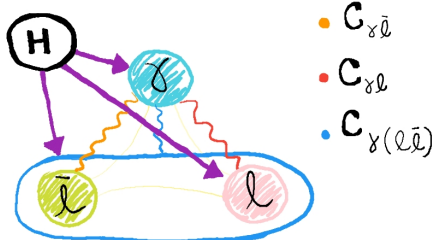
All information of the pure  $2 \otimes 2 \otimes 2$  quantum final state in

$$\begin{aligned} |\psi\rangle \simeq & \frac{-i}{N} \left( 8e \frac{Y_I}{\sqrt{2}} \kappa_{\text{CP}}^I e^{-i\delta_{\text{CP}}^I} \frac{s}{(m_h^2 - s) \sin(\theta_{\gamma I})} |+++ \rangle + a_2(m_h^2 - s) \sqrt{s} (1 + \cos(\theta_{\gamma I})) |++- \rangle \right. \\ & + b_1(m_h^2 - s) \sqrt{s} (1 - \cos(\theta_{\gamma I})) |+-+ \rangle + 8e \frac{Y_I}{\sqrt{2}} \kappa_{\text{CP}}^I e^{i\delta_{\text{CP}}^I} \frac{m_h^2}{(m_h^2 - s) \sin(\theta_{\gamma I})} |+-- \rangle \\ & + 8e \frac{Y_I}{\sqrt{2}} \kappa_{\text{CP}}^I e^{-i\delta_{\text{CP}}^I} \frac{m_h^2}{(m_h^2 - s) \sin(\theta_{\gamma I})} |-+ \rangle - a_1(m_h^2 - s) \sqrt{s} (1 - \cos(\theta_{\gamma I})) |--+ \rangle \\ & \left. - b_2(m_h^2 - s) \sqrt{s} (1 + \cos(\theta_{\gamma I})) |--- \rangle + 8e \frac{Y_I}{\sqrt{2}} \kappa_{\text{CP}}^I e^{i\delta_{\text{CP}}^I} \frac{s}{(m_h^2 - s) \sin(\theta_{\gamma I})} |--- \rangle \right) \end{aligned}$$

Multipartite systems have richer structure than bipartite ones.

# 3-qubit concurrences

fully-separable, bi-separable  
or entangled tripartite state?



## One-to-other concurrences

$$C_{i(jk)} = C_{jk|i} = \sqrt{2(1 - \text{Tr}[\rho_{jk}^2])}$$

where  $\rho_{jk}$  is the reduced density matrix of subsystem  $jk$  by tracing over particle  $i$  ( $\rho_{jk} = \text{Tr}_i[\rho]$ )

## One-to-one concurrences

$$C_{jk} = \text{Max}\{0, \eta_1^{jk} - \eta_2^{jk} - \eta_3^{jk} - \eta_4^{jk}\}$$

from eigenvalues of  $R_{jk} = \sqrt{\sqrt{\rho_{jk}}(\sigma_2 \otimes \sigma_2)\rho_{jk}^*(\sigma_2 \otimes \sigma_2)\sqrt{\rho_{jk}}}$

Coffman-Kundu-Wootters (CKW) monogamy inequality  $0 \leq t_3 = C_{jk|i}^2 - C_{ij}^2 - C_{ik}^2$

Area of concurrence triangle is a measure of the genuine entanglement

$$\mathcal{F}_3 = \sqrt{\frac{16}{3} S(S - C_{23|1})(S - C_{31|2})(S - C_{12|3})}$$

# 3-qubit Bell non-locality

LRHV or QM (or '*beyond QM*')?

Different notions of non-locality arising as extensions of the bipartite definition.

## Mermin operator

$$\mathcal{M}_3 = \hat{a}_1 \otimes \hat{b}_1 \otimes \hat{c}_2 + \hat{a}_1 \otimes \hat{b}_2 \otimes \hat{c}_1 + \hat{a}_2 \otimes \hat{b}_1 \otimes \hat{c}_1 - \hat{a}_2 \otimes \hat{b}_2 \otimes \hat{c}_2$$

to test *fully local-real theories* (no non-local correlation among any pair  $jk$  nor  $i(jk)$ )

It achieves maximum values  $\langle \mathcal{M}_3 \rangle_{\text{LRHV}} = 2$ ,  $\langle \mathcal{M}_3 \rangle_{\text{QM}} = 4$  and  $\langle \mathcal{M}_3 \rangle_{\text{alg}} = 4$ .

## Svetlichny operator

$$\begin{aligned} \mathcal{S}_3 = & \hat{a}_1 \otimes \hat{b}_1 \otimes \hat{c}_1 + \hat{a}_1 \otimes \hat{b}_1 \otimes \hat{c}_2 + \hat{a}_1 \otimes \hat{b}_2 \otimes \hat{c}_1 + \hat{a}_2 \otimes \hat{b}_1 \otimes \hat{c}_1 \\ & - \hat{a}_2 \otimes \hat{b}_2 \otimes \hat{c}_2 - \hat{a}_2 \otimes \hat{b}_2 \otimes \hat{c}_1 - \hat{a}_2 \otimes \hat{b}_1 \otimes \hat{c}_2 - \hat{a}_1 \otimes \hat{b}_2 \otimes \hat{c}_2 \end{aligned}$$

to test *bipartite local-real theories* ( $jk$  non-locally correlated but separated from  $i$ )

It achieves maximum values  $\langle \mathcal{S}_3 \rangle_{\text{LRHV}} = 4$ ,  $\langle \mathcal{S}_3 \rangle_{\text{QM}} = 4\sqrt{2}$  and  $\langle \mathcal{S}_3 \rangle_{\text{alg}} = 8$ .

**$H \rightarrow \gamma/\bar{l}$  essentially results in the same behaviour for both operators**

(some final state configurations compatible with LRHV using  $\mathcal{S}_3$  instead of  $\mathcal{M}_3$ )

# Dilepton subsystem and CP-effects

$H \rightarrow \gamma I\bar{I}$  as NLO correction of the observable dilepton decay  $H \rightarrow I\bar{I}$ .

The reduced density matrix  $\rho_{I\bar{I}}$ , neglecting the lepton mass, has vanishing polarizations  $A$  and  $B$  and the correlation matrix is independent of  $\kappa_{\text{CP}}^I$

$$C = \begin{pmatrix} \cos(2\delta_{\text{CP}}^I) \frac{2m_h^2 s}{m_h^4 + s^2} & \sin(2\delta_{\text{CP}}^I) \frac{2m_h^2 s}{m_h^4 + s^2} & 0 \\ \sin(2\delta_{\text{CP}}^I) \frac{2m_h^2 s}{m_h^4 + s^2} & -\cos(2\delta_{\text{CP}}^I) \frac{2m_h^2 s}{m_h^4 + s^2} & 0 \\ 0 & 0 & 1 \end{pmatrix}$$

The resulting concurrence is  $\mathcal{C}_{I\bar{I}} = \frac{2m_h^2 s}{m_h^4 + s^2}$ .

NO dependence on the CP-phase in this entanglement measure.

Sensitivity to  $\delta_{\text{CP}}^I$  by fitting entries of the correlation matrix, as  $H \rightarrow \tau\bar{\tau}$ .

[Fabbrichesi et al.;  
Altakach et al.]

**Concurrences are not sensitive to CP-effects**

⇒ SM computation from now on

# $H \rightarrow \gamma Z$ post-decay entanglement and *MaxEnt* Principle

Diphoton decay is maximally entangled and saturates the CHSH operator.

[Fabbrichesi et al.]

2  $\otimes$  3 system from  $H \rightarrow \gamma Z$  decay  
achieves maximal concurrence = 1  
but NO generalized-CHSH violation.

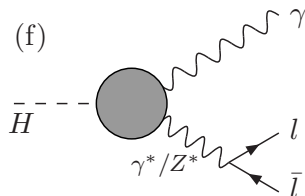
[Caban et al.; Barr; see also Bernal et al.]

$$\rho_{H \rightarrow \gamma Z} = \begin{pmatrix} 0 & 0 & 0 & 0 & 0 & 0 \\ 0 & 0 & 0 & 0 & 0 & 0 \\ 0 & 0 & 1/2 & 1/2 & 0 & 0 \\ 0 & 0 & 1/2 & 1/2 & 0 & 0 \\ 0 & 0 & 0 & 0 & 0 & 0 \\ 0 & 0 & 0 & 0 & 0 & 0 \end{pmatrix}$$

For  $\sqrt{s} \sim m_Z$  (using NWA):

$$\mathcal{M}_{(f)}^{s_1 s_2 s_3} |_{Z(OS)} \propto \sum_{\bar{s}_1} \mathcal{M}_{H \rightarrow \gamma Z}^{s_1 \bar{s}_1} \mathcal{M}_{Z \rightarrow l \bar{l}}^{\bar{s}_1 s_2 s_3}$$

Post-decay phenomenon [Aguilar-Saavedra et al.]



$$\mathcal{C}_{\gamma l | \bar{l}}^{(f)} = \mathcal{C}_{\gamma \bar{l} | l}^{(f)} = \frac{4s_w^2(1-2s_w^2)}{1-4s_w^2+8s_w^4} \approx \mathbf{0.976}$$

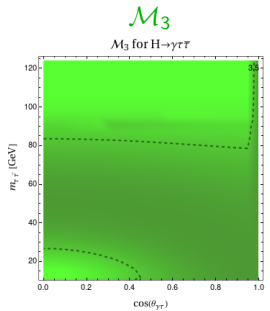
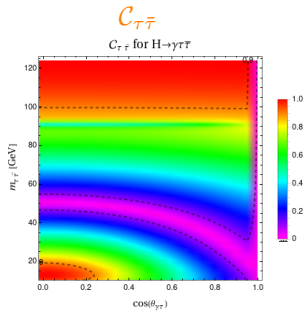
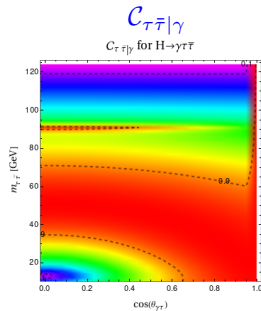
very close to the corresponding one of the  $\gamma Z$  state!

Imposeing '*MaxEnt* Principle', weak angle should satisfy  $s_w^2 = 0.25$

[Latorre et al.; Low et al.; Carena et al.; Thaller et al.]

# Tau case results

Tree level dominates above 30 GeV.



$\mathcal{C}_{\gamma\bar{\tau}|\tau}$  and  $\mathcal{C}_{\gamma\tau|\bar{\tau}}$  very close to 1.

$\mathcal{F}_3$  nearly same distribution as  $\mathcal{C}_{\tau\bar{\tau}|\gamma}$ .

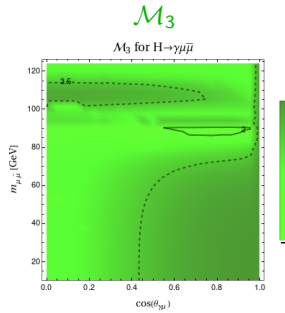
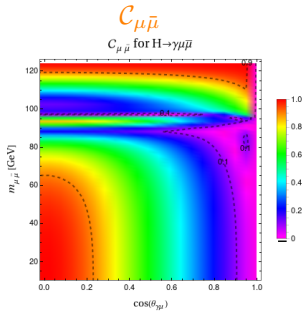
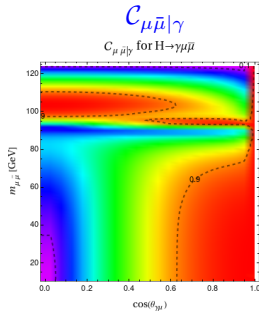
$\mathcal{C}_{\gamma\tau}$  and  $\mathcal{C}_{\gamma\bar{\tau}}$  close to 0.

$\mathcal{M}_3 > 2.8$  and close to 4 when soft photons are collinear with leptons.

# Muon case results

Tree level dominates above 100 GeV.

Distributions change respect to the tau case.



$\mathcal{C}_{\gamma\bar{\mu}|\mu}$  and  $\mathcal{C}_{\gamma\mu|\bar{\mu}}$  close to 1 but have minimum 0.6 around Z-pole.

$\mathcal{F}_3$  almost same distribution as  $\mathcal{C}_{\mu\bar{\mu}|\gamma}$  (tiny variations around Z-pole).

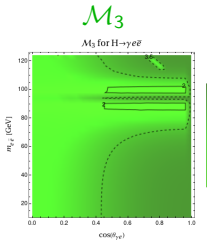
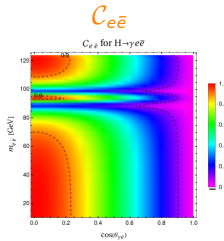
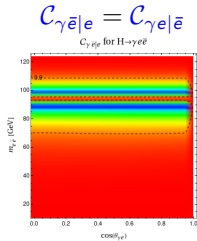
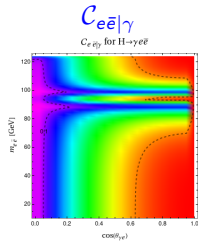
$\mathcal{C}_{\gamma\mu}$  and  $\mathcal{C}_{\gamma\bar{\mu}}$  close to 0.

Mermin operator lower than tau case with small region compatible with LR.

# Electron case results

Tree level is negligible.

Distributions change respect to the tau and muon cases.



$\mathcal{F}_3$  small variations w.r.t.  $\mathcal{C}_{e\bar{e}|\gamma}$

$\mathcal{C}_{\gamma e}$  and  $\mathcal{C}_{\gamma\bar{e}}$  close to 0.

Mermin operator similar behaviour as the muon case.

# Available experimental data for tripartite systems?

Future avenues and potential collaborations:

## Novel entanglement quantifiers accessible with current HEP data?

Other relevant tripartite decays ( $B \rightarrow K^* l\bar{l}$ ).

Actual limitation in spin measurements: incomplete quantum state tomography

⇒ Witness involving just partial information of the density matrix.

Preliminary:  $C_{Kl|l}$  just depend on  $|\mathcal{M}_{s_1 s_2 s_3}|$  (no relative complex phases)

## Non-locality test for $2 \otimes 2 \otimes 3$ systems?

such as  $t\bar{t}Z$  production or  $B \rightarrow K^* l\bar{l}$  decay

⇒ Inductive Mermin/Svetlichny construction together with  
optimal Bell inequalities of  $2 \otimes d$  systems [Bernal et al.]

# Summary

$H \rightarrow \gamma/\bar{t}$  analysis from a new perspective:

Quantify degree of entanglement and non-local correlations over the phase space of this three-body decay (3-qubit)

- Yukawa suppressed at tree-level  $\Rightarrow$  examine quantum correlations in EW 1-loop corrections.
- In general,  $\mathcal{C}_{\gamma\bar{t}|\bar{t}}$  and  $\mathcal{C}_{\gamma\bar{t}|\bar{t}}$  close to 1 and  $\mathcal{C}_{\gamma I}$  and  $\mathcal{C}_{\gamma\bar{t}}$  close to 0
- Mermin operator compatible with LR just in tiny regions for e and  $\mu$ . Quantum bound almost saturated for all families.
- CP-effects have negligible impact in this kind of observables
- Post-decay phenomenon at the Z resonance and 'MaxEnt Principle' favors weak angle close to SM value.

# Backup slides

# Kinematics for $H(p_H) \rightarrow \gamma(k)l(p_-)\bar{l}(p_+)$ decay

**Rest frame of the lepton-pair:** z-axis along the direction of the lepton, y-axis perpendicular to the decay plane and photon momentum has positive x-component.

$$p_H = \left( \sqrt{m_h^2 + |\vec{k}|^2}, |\vec{k}| \sin(\theta_{\gamma l}), 0, |\vec{k}| \cos(\theta_{\gamma l}) \right), \quad k = \left( |\vec{k}|, |\vec{k}| \sin(\theta_{\gamma l}), 0, |\vec{k}| \cos(\theta_{\gamma l}) \right),$$

$$p_- = (\sqrt{s}/2, 0, 0, \sqrt{s}\beta_l/2), \quad p_+ = (\sqrt{s}/2, 0, 0, -\sqrt{s}\beta_l/2) \text{ with } |\vec{k}| = \frac{m_h^2 - s}{2\sqrt{s}}$$

and  $\beta_l = \sqrt{1 - 4m_l^2/s}$  is the lepton velocity in this frame.

The two transverse polarization vectors of the photon are

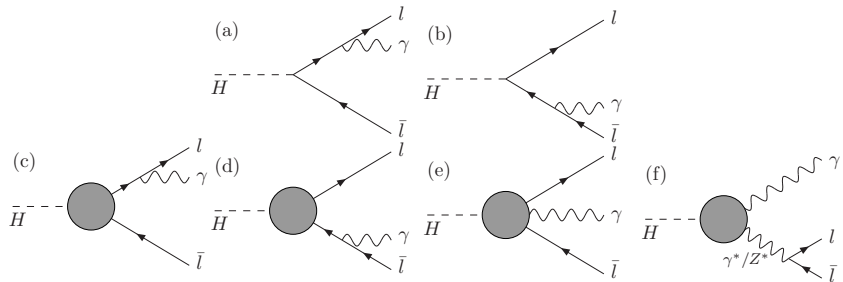
$$\varepsilon_{\pm}(k) = \frac{1}{\sqrt{2}} (0, -i \cos(\theta_{\gamma l}), \mp 1, i \sin(\theta_{\gamma l}))$$

Of course, we can choose the Higgs rest frame by performing the Lorentz transformation

$$L^{(H)} = \begin{pmatrix} \sqrt{m_h^2 + |\vec{k}|^2}/m_h & -|\vec{k}| \sin(\theta_{\gamma l})/m_h & 0 & -|\vec{k}| \cos(\theta_{\gamma l})/m_h \\ 0 & \cos(\theta_{\gamma l}) & 0 & -\sin(\theta_{\gamma l}) \\ 0 & 0 & 1 & 0 \\ -|\vec{k}|/m_h & \sqrt{m_h^2 + |\vec{k}|^2} \sin(\theta_{\gamma l})/m_h & 0 & \sqrt{m_h^2 + |\vec{k}|^2} \cos(\theta_{\gamma l})/m_h \end{pmatrix}$$

In that frame, the photon momentum is  $k^{(H)} = \left( \frac{m_h^2 - s}{2m_h}, 0, 0, \frac{m_h^2 - s}{2m_h} \right)$  and a lower cut  $E_{cut}^{\gamma}$  to the photon energy is imposed in order to avoid IR divergences in the tree level contribution. Then the upper bound on the dilepton invariant mass is obtained.

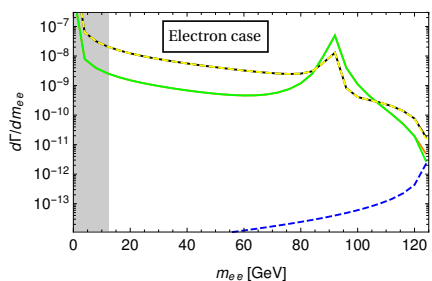
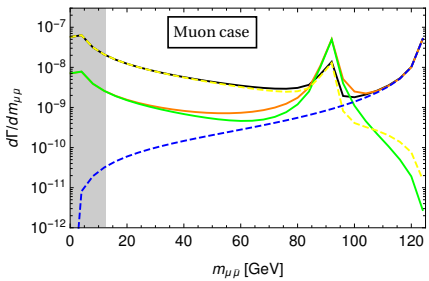
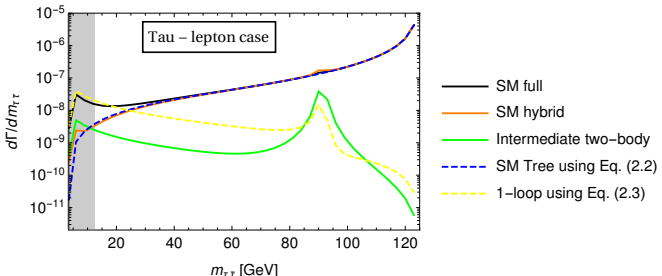
# Three-body Higgs boson decays computation



Interesting combinations

$$\begin{aligned}\mathcal{M}_{\text{full}} &= \mathcal{M}_{(a)} + \dots + \mathcal{M}_{(f)} = \mathcal{M}_{\text{Tree}} + \mathcal{M}_{\text{1-loop}}, \\ \mathcal{M}_{\text{hybrid}} &= \mathcal{M}_{(a)} + \mathcal{M}_{(b)} + \mathcal{M}_{(f)} = \mathcal{M}_{\text{Tree}} + \mathcal{M}_{(f)}, \\ \mathcal{M}_{\text{two-body}} &= \mathcal{M}_{(f)}\end{aligned}$$

# Full, hybrid and two-body contributions



$$\frac{d\Gamma_{H \rightarrow \gamma l \bar{l}}}{dm_{l\bar{l}} d\cos(\theta_{\gamma l})} = \frac{\sqrt{s - 4m_l^2(m_h^2 - s)}}{256\pi^3 m_h^3} \sum_{s_1, s_2, s_3} |\mathcal{M}_{s_1 s_2 s_3}|^2 \quad \text{where } (0.1m_h)^2 \leq s = m_{l\bar{l}}^2 \leq s_{\text{cut}} = m_h^2 - 2m_h E_{\text{cut}}^\gamma$$

# Tree level one-to-other concurrences

$$\mathcal{C}_{\gamma l|l}^{\text{Tree}} = \mathcal{C}_{\gamma \bar{l}|\bar{l}}^{\text{Tree}} = 1,$$

$$\begin{aligned}\mathcal{C}_{l\bar{l}|\gamma}^{\text{Tree}} &= \frac{\left(m_h^2 - s\right) \left(s - c_{\gamma l}^2 \left(s - 4m_l^2\right)\right)^{1/2}}{c_{\gamma l}^2 \left(4m_l^2 - s\right) \left(s \left(s - 8m_l^2 c_{\text{CP}}^2\right) + m_h^4\right) + s \left(8m_l^2 c_{\text{CP}}^2 \left(4m_l^2 - s\right) + m_h^4 - 8m_h^2 m_l^2 + s^2\right)} \times \\ &\quad \times \left(c_{\gamma l}^2 \left(4m_l^2 - s\right) \left(s \left(s - 16m_l^2 c_{\text{CP}}^2\right) + m_h^4 + 2m_h^2 s\right)\right. \\ &\quad \left.+ s \left(16m_l^2 c_{\text{CP}}^2 \left(4m_l^2 - s\right) + m_h^4 + 2m_h^2 \left(s - 8m_l^2\right) + s^2\right)\right)^{1/2}\end{aligned}$$

In the vanishing lepton mass limit,

$$\mathcal{C}_{l\bar{l}|\gamma}^{\text{Tree}}|_{m_l \ll \sqrt{s}} = \frac{m_h^4 - s^2}{m_h^4 + s^2}$$

which is very close to zero in the cut energy  $\sqrt{s}_{\text{cut}}$  and we almost have the biseparable state  $\sim (|+\rangle + |-\rangle) \otimes (|++\rangle + e^{2i\delta'_{\text{CP}}} |--\rangle)$ , where the normalization factor is omitted.

On the contrary, if the photon is collinear with lepton or antilepton,  $\mathcal{C}_{l\bar{l}|\gamma}^{\text{Tree}}$  reaches the maximal value 1.

# 1-loop one-to-other concurrences

neglecting lepton mass terms

$$\begin{aligned}\mathcal{C}_{\gamma \bar{l}|l}^{1-\text{loop}} &= \mathcal{C}_{\gamma l|\bar{l}}^{1-\text{loop}} = \\ &= \frac{2 \left( (|a_1|^2(1 - c_{\gamma l})^2 + |a_2|^2(1 + c_{\gamma l})^2)(|b_1|^2(1 - c_{\gamma l})^2 + |b_2|^2(1 + c_{\gamma l})^2) \right)^{1/2}}{(|a_1|^2 + |b_1|^2)(1 - c_{\gamma l})^2 + (|a_2|^2 + |b_2|^2)(1 + c_{\gamma l})^2}, \\ \mathcal{C}_{l \bar{l}|\gamma}^{1-\text{loop}} &= \frac{2 |a_1 b_1 (1 - c_{\gamma l})^2 - a_2 b_2 (1 + c_{\gamma l})^2|}{(|a_1|^2 + |b_1|^2)(1 - c_{\gamma l})^2 + (|a_2|^2 + |b_2|^2)(1 + c_{\gamma l})^2}\end{aligned}$$

# Genuine entanglement

Concurrence vector formalism to this 3-qubit system [Bernal et al.]  $\{q_0, q_1, q_2\} = \{0, 0, 0\}$ , neglecting lepton mass

$$\begin{aligned} q_0 &= \frac{1}{N^2} A_{\text{Tree}} \kappa'_{\text{CP}} e^{-i\delta'_{\text{CP}}} \sqrt{\frac{s}{1 - c_{\gamma l}^2}} \left( b_1(1 - c_{\gamma l})m_h^2 + b_2(1 + c_{\gamma l})s \right), \\ q_1 &= -\frac{1}{N^2} A_{\text{Tree}} \kappa'_{\text{CP}} e^{i\delta'_{\text{CP}}} \sqrt{\frac{s}{1 - c_{\gamma l}^2}} \left( a_1(1 - c_{\gamma l})m_h^2 + a_2(1 + c_{\gamma l})s \right), \\ q_2 &= \frac{1}{8N^2} \left( 64A_{\text{Tree}}^2 (\kappa'_{\text{CP}})^2 \frac{m_h^2 + s}{(m_h^2 - s)(1 - c_{\gamma l}^2)} \right. \\ &\quad \left. -(m_h^2 - s)^2 s \left( a_1 b_1 (1 - c_{\gamma l})^2 - a_2 b_2 (1 + c_{\gamma l})^2 \right) \right) \end{aligned}$$

Of course, our previous findings for either tree level or 1-loop contribution are recovered from these conditions. The  $q_0 = 0$  and  $q_1 = 0$  equations relate the form factors to each other, and  $q_2 = 0$  establish a relation between them and the tree level factors. For each kind of computation (full or two-body intermediate decay), we have non-trivial dependence of the form factors with  $s$  and  $\cos(\theta_{\gamma l})$ , and very particular kinematical configurations could correspond to biseparable states .

# One-to-one concurrences

Neglecting lepton mass terms, both photon-to-lepton  $\mathcal{C}_{\gamma l}$  and photon-to-antilepton  $\mathcal{C}_{\gamma \bar{l}}$  exactly vanish for both tree level and 1-loop contributions (then lepton mass terms in the spinors will be relevant in the numerical analysis).

The lepton-to-antilepton  $\mathcal{C}_{l \bar{l}}$  for the tree level is very compact

$$\mathcal{C}_{\gamma l}^{\text{Tree}, 1\text{-loop}}|_{m_l \ll \sqrt{s}} = \mathcal{C}_{\gamma \bar{l}}^{\text{Tree}, 1\text{-loop}}|_{m_l \ll \sqrt{s}} = 0$$

$$\mathcal{C}_{l \bar{l}}^{\text{Tree}}|_{m_l \ll \sqrt{s}} = \frac{2m_h^2 s}{m_h^4 + s^2}$$

Observe that  $\mathcal{C}_{l \bar{l}}^{\text{Tree}}$  never vanishes and is very close to 1 in the cut energy  $\sqrt{s}_{\text{cut}}$ .

# Helicity amplitudes

$$\begin{aligned}
\mathcal{M}_{+++} &= \frac{-i\sqrt{2}A_{\text{Tree}}\kappa_{\text{CP}}^I s_{\gamma I}}{(m_h^2 - s)(1 - c_{\gamma I}^2\beta_I^2)} \left( c_{\text{CP}}(m_h^2(1 - \beta_I) + s(1 + \beta_I) - 8m_I^2) + is_{\text{CP}}(m_h^2(1 - \beta_I) - s(1 + \beta_I)) \right) \\
&\quad - \frac{im_I(m_h^2 - s)s_{\gamma I}}{4\sqrt{2}} (a_1(1 - \beta_I) + a_2(1 + \beta_I) + b_1(1 + \beta_I) + b_2(1 - \beta_I)) , \\
\mathcal{M}_{++-} &= \frac{-i2\sqrt{2}A_{\text{Tree}}\kappa_{\text{CP}}^I e^{i\delta_{\text{CP}}^I}(1 + c_{\gamma I})m_I}{\sqrt{s}(1 - c_{\gamma I}^2\beta_I^2)} \\
&\quad - \frac{i(m_h^2 - s)(1 + c_{\gamma I})}{4\sqrt{2}\sqrt{s}} \left( 2a_1 m_I^2 + a_2(s(1 + \beta_I) - 2m_I^2) + b_1(s(1 - \beta_I) - 2m_I^2) + 2b_2 m_I^2 \right) , \\
\mathcal{M}_{+-+} &= \frac{-i2\sqrt{2}A_{\text{Tree}}\kappa_{\text{CP}}^I e^{i\delta_{\text{CP}}^I}(1 - c_{\gamma I})m_I}{\sqrt{s}(1 - c_{\gamma I}^2\beta_I^2)} \\
&\quad - \frac{i(m_h^2 - s)(1 - c_{\gamma I})}{4\sqrt{2}\sqrt{s}} \left( 2a_1 m_I^2 + a_2(s(1 - \beta_I) - 2m_I^2) + b_1(s(1 + \beta_I) - 2m_I^2) + 2b_2 m_I^2 \right) , \\
\mathcal{M}_{+--} &= \frac{-i\sqrt{2}A_{\text{Tree}}\kappa_{\text{CP}}^I s_{\gamma I}}{(m_h^2 - s)(1 - c_{\gamma I}^2\beta_I^2)} \left( c_{\text{CP}}(m_h^2(1 + \beta_I) + s(1 - \beta_I) - 8m_I^2) + is_{\text{CP}}(m_h^2(1 + \beta_I) - s(1 - \beta_I)) \right) \\
&\quad - \frac{im_I(m_h^2 - s)s_{\gamma I}}{4\sqrt{2}} (a_1(1 + \beta_I) + a_2(1 - \beta_I) + b_1(1 - \beta_I) + b_2(1 + \beta_I))
\end{aligned}$$

# Helicity amplitudes

$$\begin{aligned}
\mathcal{M}_{-++} &= \frac{-i\sqrt{2}\mathcal{A}_{\text{Tree}}\kappa_{\text{CP}}^I s_{\gamma I}}{(m_h^2 - s)(1 - c_{\gamma I}^2 \beta_I^2)} \left( c_{\text{CP}}(m_h^2(1 + \beta_I) + s(1 - \beta_I) - 8m_I^2) - is_{\text{CP}}(m_h^2(1 + \beta_I) - s(1 - \beta_I)) \right) \\
&\quad - \frac{im_I(m_h^2 - s)s_{\gamma I}}{4\sqrt{2}} (a_1(1 - \beta_I) + a_2(1 + \beta_I) + b_1(1 + \beta_I) + b_2(1 - \beta_I)) , \\
\mathcal{M}_{-+-} &= \frac{i2\sqrt{2}\mathcal{A}_{\text{Tree}}\kappa_{\text{CP}}^I e^{-i\delta_{\text{CP}}^I}(1 - c_{\gamma I})m_I}{\sqrt{s}(1 - c_{\gamma I}^2 \beta_I^2)} \\
&\quad + \frac{i(m_h^2 - s)(1 - c_{\gamma I})}{4\sqrt{2}\sqrt{s}} (a_1(s(1 + \beta_I) - 2m_I^2) + 2a_2m_I^2 + 2b_1m_I^2 + b_2(s(1 - \beta_I) - 2m_I^2)) , \\
\mathcal{M}_{--+} &= \frac{i2\sqrt{2}\mathcal{A}_{\text{Tree}}\kappa_{\text{CP}}^I e^{-i\delta_{\text{CP}}^I}(1 + c_{\gamma I})m_I}{\sqrt{s}(1 - c_{\gamma I}^2 \beta_I^2)} \\
&\quad + \frac{i(m_h^2 - s)(1 + c_{\gamma I})}{4\sqrt{2}\sqrt{s}} (a_1(s(1 - \beta_I) - 2m_I^2) + 2a_2m_I^2 + 2b_1m_I^2 + b_2(s(1 + \beta_I) - 2m_I^2)) , \\
\mathcal{M}_{---} &= \frac{-i\sqrt{2}\mathcal{A}_{\text{Tree}}\kappa_{\text{CP}}^I s_{\gamma I}}{(m_h^2 - s)(1 - c_{\gamma I}^2 \beta_I^2)} \left( c_{\text{CP}}(m_h^2(1 - \beta_I) + s(1 + \beta_I) - 8m_I^2) - is_{\text{CP}}(m_h^2(1 - \beta_I) - s(1 + \beta_I)) \right) \\
&\quad - \frac{im_I(m_h^2 - s)s_{\gamma I}}{4\sqrt{2}} (a_1(1 + \beta_I) + a_2(1 - \beta_I) + b_1(1 - \beta_I) + b_2(1 + \beta_I))
\end{aligned}$$

# Interesting kinematical limits

Vanishing photon energy ( $s = m_h^2$ ), the 1-loop contribution vanishes for all helicity amplitudes and the tree level yields to IR divergences for

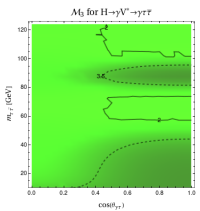
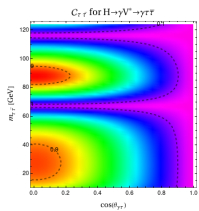
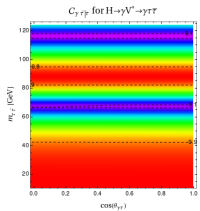
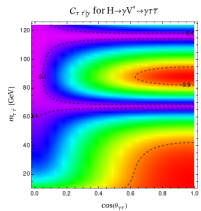
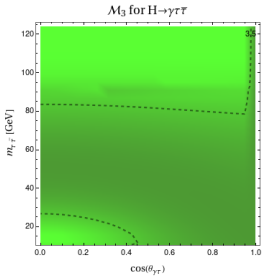
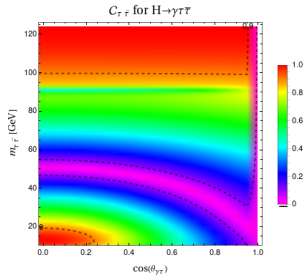
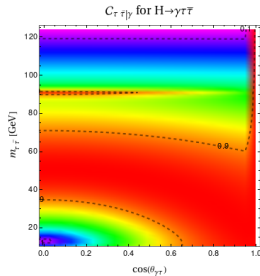
$\{+++,-+-,-++,---\}$  amplitudes (which are avoided by the lower cut  $E_{cut}^\gamma$ ).

When photon collinear with lepton ( $\theta_{\gamma l} = 0$ ) or with antilepton ( $\theta_{\gamma l} = \pi$ ), just two helicity amplitudes are non-vanishing for each case:

$$\begin{aligned}\mathcal{M}_{++-}|_{\theta_{\gamma l}=0} &= -\frac{i\sqrt{2}A_{\text{Tree}}\kappa_{\text{CP}}^I e^{i\delta_{\text{CP}}^I} \sqrt{s}}{m_l} \\ &\quad - \frac{i(m_h^2 - s)}{2\sqrt{2}\sqrt{s}} \left( 2a_1 m_l^2 + a_2(s(1 + \beta_l) - 2m_l^2) + b_1(s(1 - \beta_l) - 2m_l^2) + 2b_2 m_l^2 \right), \\ \mathcal{M}_{--+}|_{\theta_{\gamma l}=0} &= \frac{i\sqrt{2}A_{\text{Tree}}\kappa_{\text{CP}}^I e^{-i\delta_{\text{CP}}^I} \sqrt{s}}{m_l} \\ &\quad + \frac{i(m_h^2 - s)}{2\sqrt{2}\sqrt{s}} \left( a_1(s(1 - \beta_l) - 2m_l^2) + 2a_2 m_l^2 + 2b_1 m_l^2 + b_2(s(1 + \beta_l) - 2m_l^2) \right)\end{aligned}$$

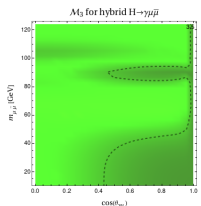
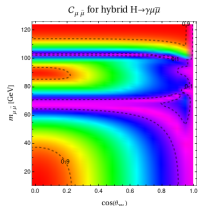
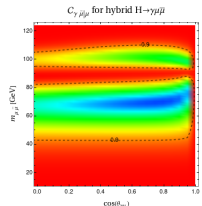
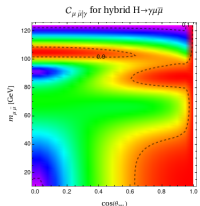
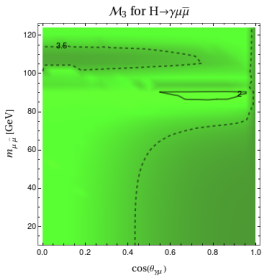
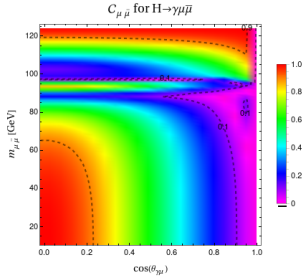
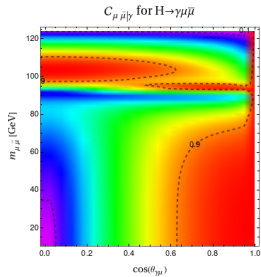
Massless lepton case ( $m_l = 0, \beta_l = 1$ ) has IR divergences when photon is collinear with lepton and antilepton.

# Tau case results for two-body computation



Full predictions similar to hybrid computation having broader regions of high entanglement than two-body case.

# Muon case results for hybrid computation



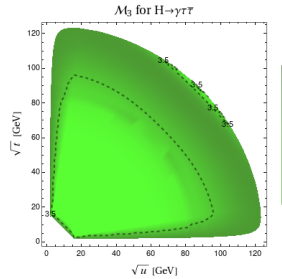
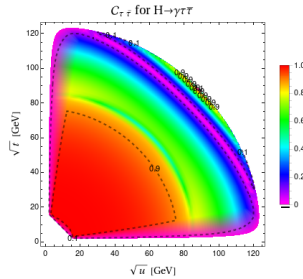
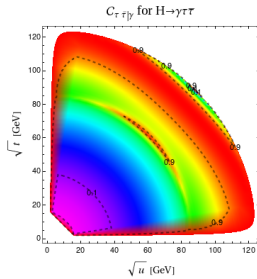
Hybrid predictions as a sort of transition between full and two-body computations reducing entanglement.

# Dalitz plots representation for $\tau$ case

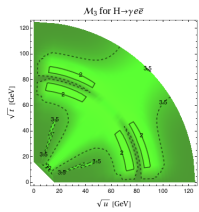
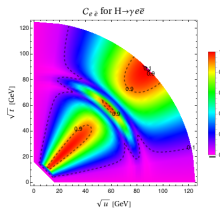
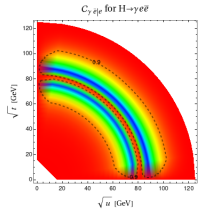
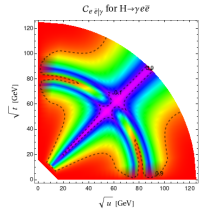
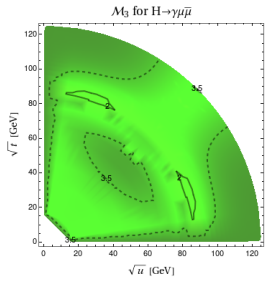
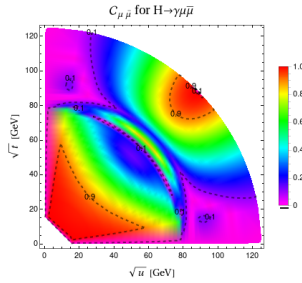
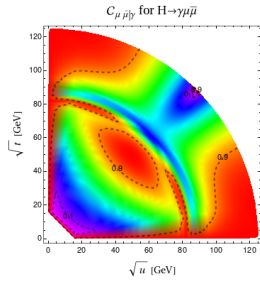
Change of variables  $\cos(\theta_{\gamma l}) = \frac{u-t}{(m_h^2-s)\sqrt{1-4m_l^2/s}} \Rightarrow$

frame independent representation using Mandelstam variables

$$s = (p_- + p_+)^2, t = (k + p_-)^2 \text{ and } u = (k + p_+)^2$$



# Dalitz plots representation for $e$ and $\mu$ cases



# Testing non-locality at colliders

**Using Bell inequalities at colliders to test non-locality is challenging** due to the difficulty in measuring the final state's non-commuting observables.

Issues to conduct a loophole-free test of local realism at conventional collider experiments [Abel et al.; Horodecki et al.]:

*Detection loop-hole:* high-energy collider experiments have imperfect acceptance and detection efficiency

*Freedom-of-choice loophole:* we do not have the freedom to choose the spin measurement axes, as the spin measurement is constituted indirectly and statistically by analysing the momentum distributions.

*There is always some hidden variable theory that can explain the observed momentum data* since momenta of observed particles are essentially commuting observables.

**The interest of this work is not a high-energy test of local realism!!!**

# Three-body $B$ meson decays

Processes  $B \rightarrow K^{*0}l\bar{l}$  and  $\bar{B} \rightarrow \bar{K}^{*0}l\bar{l}$  with final state in the helicity amplitude basis  $\{+, 0, -\} \otimes \{+, -\} \otimes \{+, -\}$ :

$$|\psi\rangle = \mathcal{H}_{++-}|++-\rangle + \mathcal{H}_{+-+}|+-+\rangle + \mathcal{H}_{0+-}|0+-\rangle + \mathcal{H}_{0-+}|0-+\rangle + \mathcal{H}_{-+-}|-+-\rangle + \mathcal{H}_{--+}|--+\rangle$$

We found one-to-other concurrences (NOT accessible with current data)

$$\begin{aligned} \mathcal{C}_{\bar{K}^*I^+|I^-} &= \mathcal{C}_{\bar{K}^*I^-|I^+} = \\ &= 2 \left( \frac{d\Gamma}{dq^2} \right)^{-1} \left( |\mathcal{A}_0^L|^2 + |\mathcal{A}_\perp^L|^2 + |\mathcal{A}_\parallel^L|^2 \right)^{1/2} \left( |\mathcal{A}_0^R|^2 + |\mathcal{A}_\perp^R|^2 + |\mathcal{A}_\parallel^R|^2 \right)^{1/2} \end{aligned}$$

$$\begin{aligned} \mathcal{C}_{I^-I^+|\bar{K}^*} &= \\ &= 2 \left( \frac{d\Gamma}{dq^2} \right)^{-1} \left( |\mathcal{A}_0^L|^2 |\mathcal{A}_\perp^R|^2 + |\mathcal{A}_0^R|^2 |\mathcal{A}_\perp^L|^2 - 2 |\mathcal{A}_0^L| |\mathcal{A}_0^R| |\mathcal{A}_\perp^L| |\mathcal{A}_\perp^R| \cos(\phi_0^L - \phi_0^R - \phi_\perp^L + \phi_\perp^R) \right. \\ &\quad \left. + |\mathcal{A}_0^L|^2 |\mathcal{A}_\parallel^R|^2 + |\mathcal{A}_0^R|^2 |\mathcal{A}_\parallel^L|^2 - 2 |\mathcal{A}_0^L| |\mathcal{A}_0^R| |\mathcal{A}_\parallel^L| |\mathcal{A}_\parallel^R| \cos(\phi_\parallel^L - \phi_\parallel^R - \phi_0^L + \phi_0^R) \right. \\ &\quad \left. + |\mathcal{A}_\perp^L|^2 |\mathcal{A}_\parallel^R|^2 + |\mathcal{A}_\perp^R|^2 |\mathcal{A}_\parallel^L|^2 - 2 |\mathcal{A}_\perp^L| |\mathcal{A}_\perp^R| |\mathcal{A}_\parallel^L| |\mathcal{A}_\parallel^R| \cos(\phi_\perp^L - \phi_\perp^R - \phi_\parallel^L + \phi_\parallel^R) \right)^{1/2} \end{aligned}$$

$$\text{where } \mathcal{A}_\perp^{L(R)} = \frac{\mathcal{H}_{-+-}(++) - \mathcal{H}_{--+}(-+-)}{\sqrt{2}}, \quad \mathcal{A}_\parallel^{L(R)} = \frac{\mathcal{H}_{-+-}(++) + \mathcal{H}_{--+}(-+-)}{\sqrt{2}}, \quad \mathcal{A}_0^{L(R)} = \mathcal{H}_{0-+}(0+-)$$